Advances in
Bridge Engineering

ORIGINAL INNOVATION Open Access

Stochastic analysis for bending capacity of precast prestressed concrete bridge piers using Monte-Carlo simulation and gradient boosted regression trees algorithm

Xiaopan Lai[1], Zhao Lu[1], Xinyu Xu[1] and Chuanjin Yu[2,3*]

*Correspondence:
ycj@swjtu.edu.cn

[1] Railway Eryuan Engineering Group Co., Ltd., Chengdu, Sichuan 610031, P. R. China
[2] Wind Engineering Key Laboratory of Sichuan Province, Southwest Jiaotong University, Chengdu, Sichuan 610031, P. R. China
[3] National Key Laboratory of Bridge Intelligent and Green Construction, Southwest Jiaotong University, Chengdu, Sichuan 611756, P. R. China

Abstract

The use of precast prestressed concrete bridge piers is rapidly evolving and widely applied. Nevertheless, the probabilistic behavior of the bending performance of precast prestressed concrete bridge piers has often been overlooked. This study aims to address this issue by utilizing actual precast bridge piers as the engineering context. Through the implementation of the Monte-Carlo simulation and Gradient Boosted Regression Trees (GBRT) algorithm, the stochastic distribution of the bending performance and their critical factors are identified. The results show that the normal distribution is the most suitable for the random distribution of bending performance indicators. The variability of the elastic modulus of ordinary steel bars, initial strain of prestressed steel hinge wires, and constant load axial force has little effect on the bending moment performance, while the yield stress of ordinary steel bars, elastic modulus of concrete, compressive strength of unrestrained concrete, and elastic modulus of prestressed steel hinge wires have a greater impact on the bending performance. Additionally, the compressive strength of unrestrained concrete has a significant influence on the equivalent bending moment of the cross-section that concerns designers.

Keywords: Prefabricated assembled, Prestressed concrete bridge piers, Stochastic simulation, Probability distribution characteristics, Influencing factors

1 Introduction

The upper structures of Chinese railway bridges have extensively utilized prefabrication techniques, which have significantly improved construction efficiency and project quality (Zhao et al. 2022). However, construction of the lower structures still relies heavily on manual steel reinforcement and on-site concrete pouring, hindering the development of industrialized and intelligent construction levels of railway bridge construction. It is imperative to carry out research on the prefabrication and assembly of bridge piers, which conform to the current trend of green, efficient, and low-carbon bridge structures, as they offer advantages such as saving on formwork, occupying less space, faster

construction speed, and improved construction safety (Aydın and Ayvaz 2013; Zhang and Alam 2020).

The piers of bridges are the vulnerable parts of bridge structures during earthquakes. Although the development of precast prestressed concrete piers is rapid, their seismic performance is still an important bottleneck that restricts their widespread use (Fahmy et al. 2023). In order to explore the seismic performance of the mechanical properties of precast prestressed concrete pier's bending behavior, numerous scholars have carried out research using mainstream methods such as numerical simulation (Wang and Li 2022; Qu et al. 2018), quasi-static test (Palermo 2016; White and Palermo 2016), and vibration table test (Zhanghua et al. 2020; Mehrsoroush et al. 2017). However, these efforts have not yet focused on the stochastic characteristics of structural response under earthquake action.

It is imperative to evaluate the reliability of piers subjected to seismic forces, given the significant degree of randomness in earthquake actions and the numerous uncertain factors present in bridge structural design. Scholars have thoroughly investigated methods for analyzing structural reliability for different types of bridge pier. To study the safety of an existing pier of a railway bridge, a reliability analysis of random variables was conducted with special attention under concrete fatigue conditions (Abishek and Nageswara 2019). For probabilistic-based design approaches of bridge piers, concerning the trade-off between safety and cost, a method through minimizing the structural cost function at different design lifetimes and calculates the reliability level of bridge piers subjected to flexural and axial failure modes under extreme seismic events is presented (Safari et al. 2021). It analyzes the reliability of a bridge pier rocking shallow foundation system under earthquake loads using Monte Carlo simulation and response surface method, and finds that the system's performance improves during strong earthquakes (Deviprasad et al. 2022). Previous research has predominantly concentrated on cast-in-place piers. However, the seismic performance of prefabricated and assembled bridge piers is significantly different from that of monolithic cast-in-place bridge piers due to the existence of joint structures (Wang et al. 2009). There is not much research on the reliability of precast piers under earthquake loads.

Regarding of the reliable analysis methods, many scholars have also devoted significant effort to this topic. To improve the efficiency of seismic reliability analysis for multi-span bridge piers, this reference examines the advantages of the adaptive response surface method based on the moving least squares approach over the conventional response surface method that typically employs the least squares approach (Ghosh et al. 2018). Results show that the former exhibits higher efficiency and accuracy, and can evaluate the seismic reliability of multi-span bridge piers by comparing nonlinear time history analysis results with fiber sections of ground motion corresponding to the specified seismic hazard level. Data-driven metamodeling has also been utilized to approximate structural response and consider uncertainties. The vulnerability curves of reinforced concrete highway bridge piers were extracted using this approach to demonstrate its high efficiency and accuracy (Hoang et al. 2021). A combined method based on the maximum entropy principle, fractional moments, partially stratified sampling, and Nataf transformation is proposed for seismic reliability analysis of bridges with uncertainties, with focus given to evaluating the impact of random variable correlation on the seismic

reliability of high-pier continuous rigid frame bridges (Chen et al. 2021). Nevertheless, the aforementioned techniques have yet to quantitatively determine the random parameters that significantly affect the structural performance during seismic loading.

At present, research on the reliability of prefabricated bridge piers under earthquake conditions is limited. Moreover, the M-ϕ curve, which is commonly utilized in seismic analysis, depicts the ductility behavior of a structural element (Shi et al. 2007) and can be used to indirectly observe the structural ductility under earthquake loads. Consequently, this research concentrates on the stochastic behavior of the bending capacity of precast bridge piers with unbonded prestressed steel, which is vital in improving the overall stability of precast pier structures and mitigating residual displacements induced by earthquakes (Fu et al. 2023). Furthermore, the study endeavors to examine the random parameters that influence the structural performance under seismic loads. In particular, this study scrutinizes the effects of various random parameters on a precast prestressed bridge pier situated in a specific railway elevated segment. These parameters include the elastic modulus and yield stress of ordinary steel, the elastic modulus and unconfined compressive strength of concrete, the elastic modulus of prestressed steel hinge line, the initial strain, and the constant axial force due to loading. This approach relies on a hybrid model that combines the Monte Carlo method with a Gradient Boosting Regression Tree (GBRT) model to analyze various performance indicators of section bending, including longitudinal initial yield moment and sectional curvature of ordinary steel, ultimate moment, sectional ultimate curvature, curvature ductility, equivalent yield moment, and equivalent yield sectional curvature. By determining the probability distribution characteristics and crucial influencing factors of these performance indicators, the research provides a foundation for utilizing dependable design methods for ensuring the safety assessment of bridges.

The subsequent sections of the paper are organized as follows. Section 2 presents an overview of material constitutive relationship and stochastic features. Section 3 focuses on the methods used for calculating and analyzing the bending properties of cross-sections. Section 4 delves into the random characteristics of section bending performance. Finally, Section 5 presents the concluding remarks.

2 Material constitutive relationship and stochastic features

The mechanical behavior of materials can be described by the material constitutive relationship, which reveals the stress–strain relationship of the material under different load conditions. In practical engineering applications, the stress–strain relationship of materials exhibits strong stochastic features due to factors such as the randomness of the material's microscopic structure, environmental variables, and uncertainty in loading conditions.

2.1 Steel reinforcement

The stress–strain relationship of steel reinforcement is an important aspect in the study of the mechanical properties of concrete structures. Taking HRB400 ordinary steel reinforcement as an example, its stress–strain relationship is shown in Fig. 1 and can be divided into four stages: elastic stage, yield stage, strengthening stage,

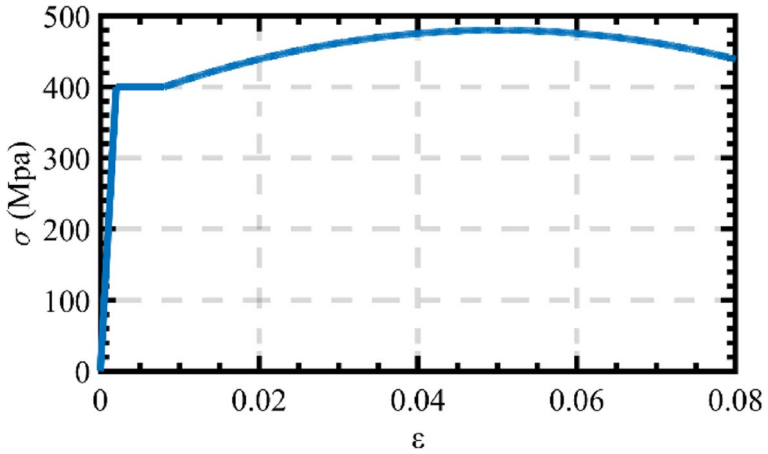

Fig. 1 The stress–strain relationship of steel reinforcement

and necking stage. In this study, the ultimate tensile strain of the steel reinforcement is set to a fixed value of 0.02.

2.2 Concrete

In terms of the study of constitutive models for confined concrete, numerous domestic and foreign scholars have made significant efforts and proposed their own stress–strain equations for different types of confined concrete. In this study, the Mander constitutive model is adopted for confined concrete (Mander et al. 1988a, 1988b). Its stress–strain relationship is described as Eq. (1) to Eq. (5).

$$f_c = \frac{f_{cc} x r}{r - 1 + x^r} \tag{1}$$

$$x = \frac{\varepsilon_c}{\varepsilon_{cc}} \tag{2}$$

$$\varepsilon_{cc} = \varepsilon_{c0}\left[1 + 5\left(\frac{f_{cc}}{f_{co}} - 1\right)\right] \tag{3}$$

$$r = \frac{E_c}{E_c - E_{sec}} \tag{4}$$

$$E_{sec} = \frac{f_{cc}}{\varepsilon_{cc}} \tag{5}$$

in which f_{cc} and ε_{cc} represent the peak stress and corresponding strain of confined concrete, while f_{co} and ε_{co} represent the peak stress and corresponding strain of unconfined concrete. E_c and E_{sec} are respectively the initial modulus of concrete and the secant modulus corresponding to the peak stress of confined concrete.

2.3 Random characteristics

The random characteristics of materials refer to the irregularities or unpredictabilities present in their structure. These features can stem from various factors such as the material's preparation process, composition, and external environment. They manifest as irregularities in form, such as lattice distortion, defects, and dislocations, as well as differences in chemical composition, morphology, and size that give rise to variability. Such random features significantly impact the mechanical properties of materials.

In comparison to the mechanical parameters of ordinary steel bars, the variation in the mechanical parameters of concrete is greater. The variation coefficients of the elastic modulus E_s and yield strength f_y of ordinary steel bars are 0.04 and 0.1, respectively, and both follow a normal distribution (Fahmy et al. 2023). The variation coefficient of the elastic modulus E_c of concrete is 0.3, while the variation coefficient of the unconfined compressive strength f_{c0} of concrete is 0.2, both following a normal distribution (Hoang et al. 2021). The variation coefficients of the elastic modulus E_p and initial strain ε_{p0} of prestressed steel hinge wires are both 0.2 and follow a normal distribution. Furthermore, the constant load axial force N_g is subject to a normal distribution with a coefficient of variation of 0.015. All the stochastic parameters have been summarized in Table 1.

3 Bending properties of cross-sections calculations

In this context, the basic procedure for calculating the bending performance indicators of the cross-section is introduced. On this basis, multiple probability density functions that describe the random distribution of bending performance indicators are presented, along with the process of utilizing GBRT model to analyze the importance of factors that influence the bending performance of the cross-section.

3.1 Typical design parameters

Precast assembled bridge piers were utilized in a specific section of the railway transit viaduct. The Fig. 2 below depicts the typical cross-section of the precast assembled bridge pier, exhibiting a 1.6 m wide section along the bridge, and a 2.8 m width transverse to the bridge. HRB400 standard steel bars, measuring 25 mm in diameter, are uniformly situated along both the longitudinal and transverse directions. The section contains four apertures for prestressed conduits, each with a total area of 2100 mm^2. Table 2 depicts the primary design components of the pier and its key performance indicators.

Table 1 Random characteristics of various parameters

Random variable	Meaning	Distribution	Variation
E_s	Elastic modulus of ordinary steel bars	Normal distribution	0.04
f_y	Yield strength of ordinary steel bars	Normal distribution	0.1
E_c	Elastic modulus of concrete	Normal distribution	0.3
f_{co}	Unconfined compressive strength of concrete	Normal distribution	0.2
E_p	Elastic modulus of prestressed steel hinge wires	Normal distribution	0.2
ε_{p0}	Initial strain of prestressed steel hinge wires	Normal distribution	0.2
N_g	Constant load axial force	Normal distribution	0.015

Table 2 Primary Components and its key performance indicators

Primary Components	Specifications	Key performance indicators
Longitudinal reinforcement	HRB400	$f_y = 400$ MPa $E_s = 200$GPa
Concrete for pier body	C40	$f_{c0} = 40$ MPa $E_c = 34$GPa
Vertical Non-Adhesive Prestressed Steel Strand	Nominal diameter Φ^s15.2	$f_{pk} = 1860$ MPa $E_p = 195$GPa $\varepsilon_{p0} = 0.00668$

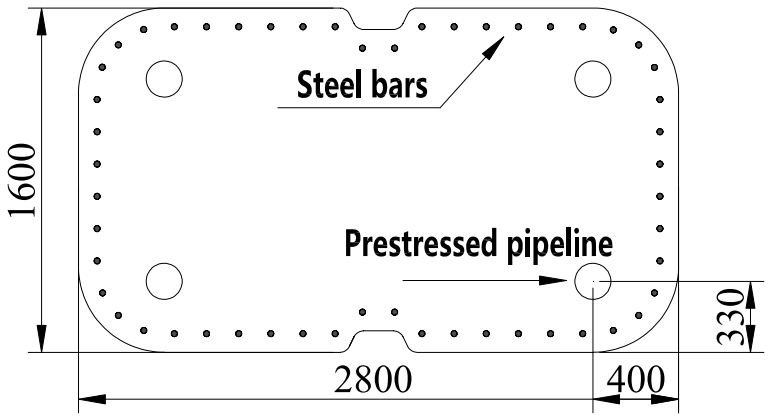

Fig. 2 Typical cross-section of a precast assembled bridge pier (unit: mm)

3.2 Sectional bending strength and curvature

In order to examine the bending performance of precast segmental prestressed concrete bridge piers under ultimate failure, an analysis of the M-ϕ curve is first conducted. The specific calculation process can be found in the reference (Technical standard for prefabricated bridge piers of rail transit 2020). The initial yield bending moment M_{yo} and the initial yield sectional curvature ϕ_{yo} of longitudinal ordinary steel bars are defined, and the maximum bearing bending moment is taken as the ultimate bending moment M_{yl}. When the compressive zone reaches the maximum compressive strain ε_{cu} of concrete, the section reaches a limit state, with the sectional curvature being the ultimate curvature ϕ_{cu}. Furthermore, the curvature ductility μϕ of the section can be calculated using Eq. (6).

$$\mu_{\varphi} = \frac{\varphi_{cu}}{\varphi_y} \tag{6}$$

To determine the equivalent yield bending moment M_y and the equivalent yield curvature ϕ_y of the section based on the M-ϕ curve, the equal area method is used. For designers, the equivalent yield bending moment M_y is a critical indicator of sectional performance. Both the calculation of the M-ϕ curve and the equivalent bending moment require trial calculations. To improve computational efficiency, this study

implements a binary search algorithm in actual calculations. This method can effectively reduce computation time and increase calculation accuracy.

3.3 Randomness of bending performance

The bending performance of a section is closely related to the material properties. As the material properties are random, the bending performance of the section also changes accordingly. In this study, a large number of random parameters are generated based on the Monte Carlo method, and the M-ϕ curve and equivalent yield moment My are analyzed to obtain corresponding random samples of sectional performance indicators. Next, common probability density functions are used to fit various bending indicators, and the optimal distribution function types are determined. Five probability density functions are employed in this study, including normal distribution, lognormal distribution, generalized extreme value distribution, gamma distribution, and Weibull distribution, as shown in Table 3.

3.4 Importance analysis

To investigate the influence of random parameters on various indicators of sectional bending performance, this study will utilize the GBRT model. GBRT is a supervised learning method based on decision trees, which iteratively increases the number of fitted trees to improve prediction accuracy and can be expressed using Eq. (7) When compared to a single decision tree, the GBRT model exhibits higher accuracy and better generalization ability.

$$F_m(x) = F_{m-1}(x) + \gamma_m h_m(x) \tag{7}$$

Here, $F_m(x)$ represents the model output after the mth iteration, $F_{m\text{-}1}(x)$ represents the model output after the (m-1)th iteration, γ_m represents the step size for the mth tree, and $h_m(x)$ represents the output of the mth tree.

As an example, the GBRT can be used to construct a predictive model to forecast the influence of random parameters on the equivalent yield bending moment M_y. Specifically, this predictive model can be implemented using Eq. (8).

Table 3 Random characteristics of material parameters

Distribution	Symbols	Probability density function (PDF)
Normal distribution	Normal	$f(x) = \frac{1}{\sigma\sqrt{2\pi}} e^{-\frac{(x-\mu)^2}{2\sigma^2}}$
Lognormal distribution	Lognormal	$f(x) = \frac{1}{x\sigma\sqrt{2\pi}} e^{-\frac{(\ln x-\mu)^2}{2\sigma^2}}$
Generalized extreme value distribution	GEV	$f(x) = \frac{1}{\sigma}\left[1+\xi\left(\frac{x-\mu}{\sigma}\right)\right]^{-\frac{1}{\xi}-1} e^{-\left[1+\xi\left(\frac{x-\mu}{\sigma}\right)\right]^{-\frac{1}{\xi}}}$
Gamma distribution	Gamma	$f(x) = \frac{\beta^\alpha}{\Gamma(\alpha)} x^{\alpha-1} e^{-\beta x}$
Weibull distribution	Weibull	$f(x) = \begin{cases} \frac{k}{\lambda}\left(\frac{x}{\lambda}\right)^{k-1} e^{-(x/\lambda)^k}, x \geq 0 \\ 0, x < 0 \end{cases}$

In the formulas above, μ represents the mean, σ represents the standard deviation, ξ represents the shape parameter, α and β are parameters of the Gamma distribution, and k and λ are parameters of the Weibull distribution

$$M_y = \mathrm{GBRT}\left(E_s, f_y, E_c, f_{co}, E_p, \varepsilon_{p0}, N_g\right) \tag{8}$$

Meanwhile, each decision tree in the GBRT model provides a feature importance degree. The calculation of feature importance is achieved by randomly sampling each feature without replacement and calculating the splitting contribution of that feature at each node. The specific calculation process is shown in Eq. (9).

$$Importance_j = \frac{\sum_{t=1}^{T} I\left(j \in T_t\right) \cdot Gain(t)}{\sum_{t=1}^{T} Gain(t)} \tag{9}$$

Here, $I(j \in T_t)$ is an indicator function that takes a value of 1 when feature j is selected as the splitting node in the tth decision tree, and 0 otherwise. Gain(t) represents the reduction in the loss function for the tth decision tree.

As an example, in this study there are a total of 7 random parameters that influence the equivalent yield bending moment M_y. For each feature, its importance degree in affecting the equivalent yield bending moment M_y can be normalized and calculated using Eq. (10).

$$Importance_j = \frac{Importance_j}{\sum_{i=1}^{7} Importance_i} \tag{10}$$

4 Random characteristics analysis

4.1 Probability distribution

Based on the random material properties shown in Table 1, this study used Monte Carlo sampling techniques to calculate the M-ϕ curve of a typical precast assembled bridge pier section, obtaining 6000 random samples of seven key indicators: M_{yo}, ϕ_{yo}, M_{yl}, ϕ_{cu}, μ_ϕ, M_y and ϕ_y. Based on these samples, typical probability distribution functions listed in Table 2 were fitted for each indicator, as shown in Figs. 3, 4, 5, 6, 7, 8 and 9. Table 4 presents the goodness-of-fit for different probability distribution functions.

Specifically, in the Weibull distribution, only the goodness-of-fit for ϕ_{cu} exceeds 0.98. The situation is similar for the lognormal distribution, where only the goodness-of-fit for M_{yo} and ϕ_y exceed 0.98, while the fitting performance for other indicators is relatively poor. In the Gamma distribution, the goodness-of-fit for M_{yo}, ϕ_{yo} and ϕ_{cu} all exceed 0.98. In the Generalized Extreme Value distribution, the goodness-of-fit for M_{yo}, ϕ_{cu}, μ_ϕ and ϕ_y all exceed 0.98, indicating that this distribution has strong descriptive capabilities for these indicators. In the normal distribution, the goodness of fit for the six key indicators—M_{yo}, ϕ_{yo}, M_{yl}, ϕ_{cu}, M_y and ϕ_y—exceeded 0.98.

Among the five distributions, the normal distribution shows the best fitting performance, followed by the Generalized Extreme Value distribution and Gamma distribution. The goodness-of-fit for the lognormal distribution and Weibull distribution

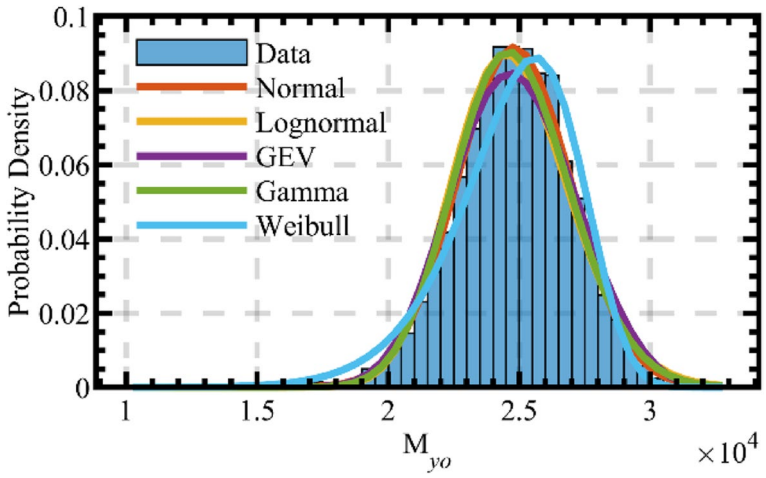

Fig. 3 Probability Density Distribution Curve for M_{yo}

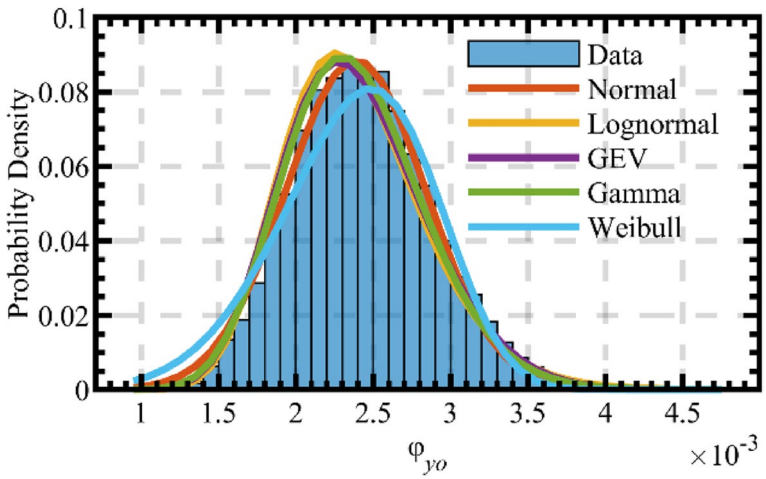

Fig. 4 Probability Density Distribution Curve for φ_{yo}

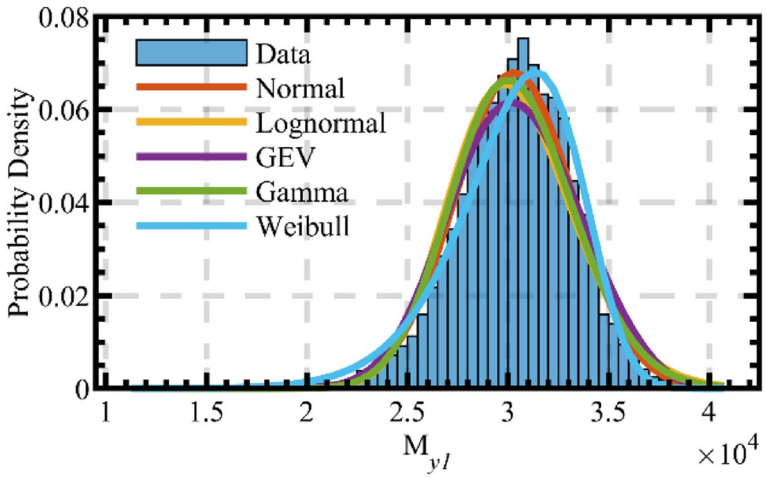

Fig. 5 Probability Density Distribution Curve for M_{yl}

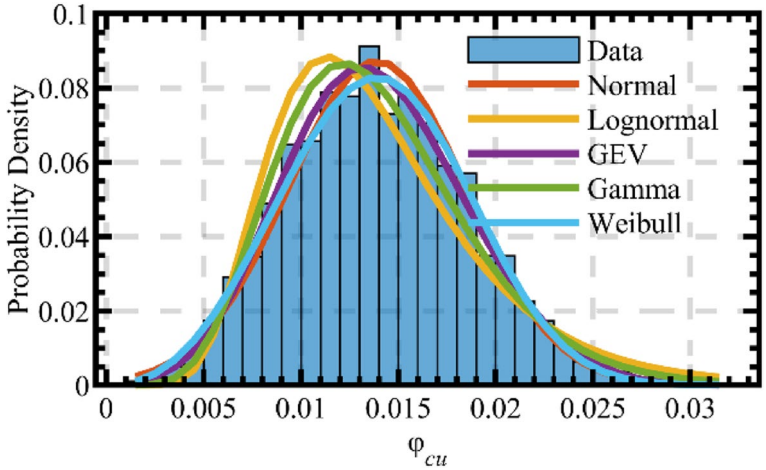

Fig. 6 Probability Density Distribution Curve for φ_{cu}

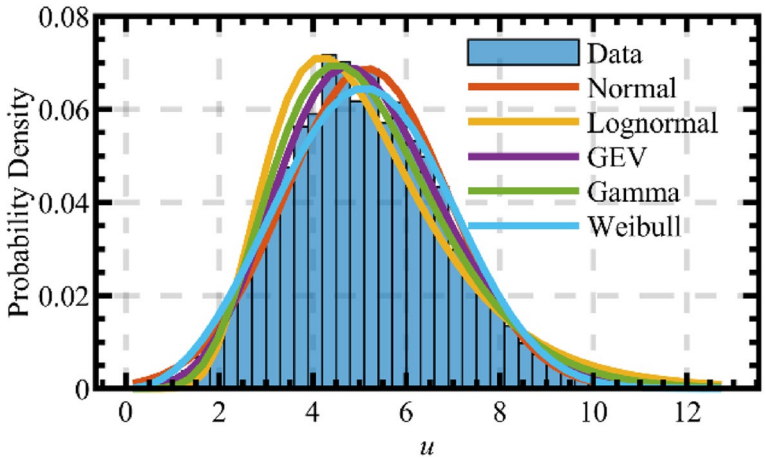

Fig. 7 Probability Density Distribution Curve for u

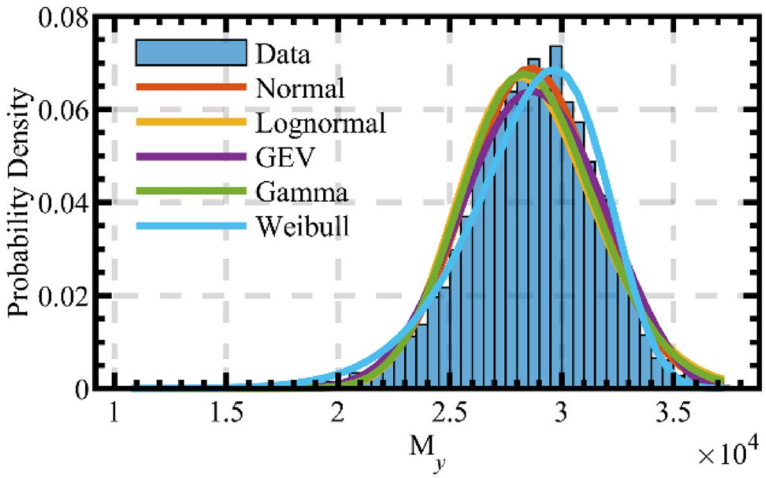

Fig. 8 Probability Density Distribution Curve for M_y

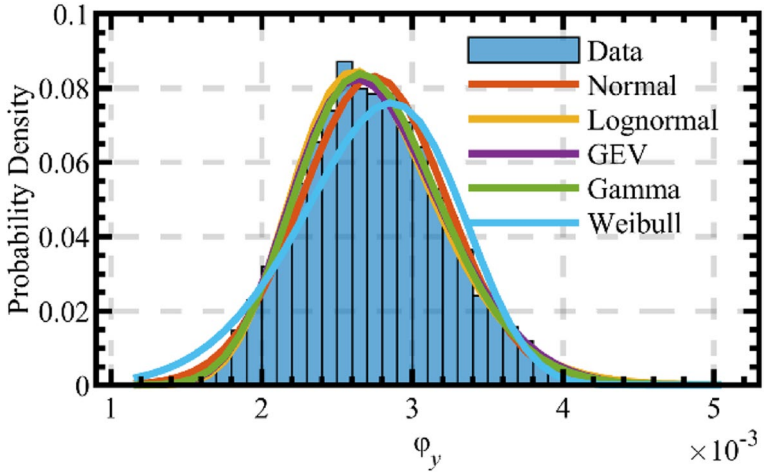

Fig. 9 Probability Density Distribution Curve for φ_y

Table 4 Goodness of fit of various probability density functions for the performance indicator of cross-sectional bending moment

	M_{yo}	φ_{yo}	M_{yl}	φ_{cu}	μ_{φ}	M_y	φ_y
Normal	**0.9954**	**0.9943**	**0.9841**	0.9817	0.9773	**0.9894**	0.9891
Lognormal	0.9814	0.9697	0.9534	0.9119	0.9434	0.9636	0.9914
GEV	0.9803	0.9781	0.9541	**0.9873**	**0.9907**	0.9786	0.9948
Gamma	0.9876	0.9839	0.966	0.9609	0.9797	0.9745	**0.9962**
Weibull	0.9652	0.9639	0.977	0.9857	0.9785	0.976	0.9395

For different indicators, the optimal goodness of fit value is highlighted in bold black

Table 5 Goodness of fit of cross-sectional bending moment performance indicator using the GBRT model

	M_{yo}	φ_{yo}	M_{yl}	φ_{cu}	μ_{φ}	M_y	φ_y
R^2	0.9856	0.9897	0.9878	0.9824	0.9836	0.9511	0.9691

is relatively low, indicating poor applicability. Therefore, for the random characteristics description of the section bending performance of precast prestressed concrete bridge piers, the normal distribution can be adopted.

4.2 Crucial factors

In order to investigate the effects of different materials and random load characteristics on sectional bending moment performance, a GBRT model was established for each bending performance indicator of the section to examine the importance of different random parameters on the sectional bending moment performance indicators. In order to verify the fitting performance of the model, the goodness of fit R^2 was used for evaluation, as shown in Table 5. The goodness of fit R^2 for all sectional bending moment indicators is greater than 0.95, indicating that the established model can accurately predict the impact of different random variables on sectional bending moment performance.

Figure 10 shows the degree of influence of each random parameter on specific indicators of sectional bending moment performance. Taking the initial yield bending moment of longitudinal ordinary steel bar M_{yo} as an example, the first column represents the importance of the seven random variables to M_{yo}, with a total sum of 1, and the depth of color represents the importance of the influencing factor. The results show that the yield stress f_y of ordinary steel bar has a significant impact on the initial yield curvature ϕ_{yo} and equivalent yield curvature ϕ_y of longitudinal ordinary steel bars, with importance values of 0.90 and 0.85 respectively. The other five sectional indicators M_{yo}、M_{yl}、ϕ_{cu}、μ_ϕ and M_y, the elastic modulus of concrete E_c, the compressive strength f_{co} of unconstrained concrete, and the elastic modulus E_p of prestressed steel hinge lines also have notable impacts. Among them, the compressive strength f_{co} of unconstrained concrete has the highest importance value, all of which are above 0.5. For the equivalent yield bending moment M_y that is most concerned by designers, the importance value of the compressive strength f_{co} of unconstrained concrete is 0.51, significantly higher than other influencing factors.

Therefore, for sectional bending moment indicators, the yield stress f_y of ordinary steel bars, the elastic modulus of concrete E_c, the compressive strength f_{co} of unconstrained concrete, and the elastic modulus E_p of prestressed steel hinge lines are the most important factors affecting sectional bending moment performance indicators. The elastic modulus E_s of ordinary steel bars, the initial strain ε_{p0} of prestressed steel hinge lines, and the constant load axial force N_g all have importance values of less than 0.1, indicating that these variation coefficients have relatively small impacts on sectional bending moment performance. It should be noted that this does not mean that these parameters are unimportant, but only that their impact is relatively small under the current circumstances and still need to be considered in the design process.

Fig. 10 The influence degree of random parameters on sectional bending moment performance

5 Conclusion

Drawing from practical engineering experience, this research employs a stochastic analysis to determine the bending performance of prestressed concrete bridge piers, taking into account variable random parameters. The study thoroughly examines the distribution of the section's bending performance indicators and the crucial factors. The conclusions of the study are as follows.

1 The optimal fit for the stochastic distribution of prestressed concrete bridge pier bending performance indicators is demonstrated by the normal distribution.
2 The variability of the elastic modulus of ordinary steel bars, the initial strain and constant axial load of prestressed steel hinge wires have little effect on the bending moment performance of the section. On the other hand, the yield strength of ordinary steel bars, the elastic modulus of concrete, the compressive strength of unconstrained concrete, and the elastic modulus of prestressed steel hinge wires are important factors affecting the bending performance indicators of the section. For the equivalent bending moment of the section, the compressive strength of unconstrained concrete has the greatest influence.

It should be noted that this study only starts from the design perspective and uses standard calculation formulas for research. In a real environment, the bending performance of the designed section still needs to be further verified through model tests.

Acknowledgements
The authors are grateful for the China Postdoctoral Science Foundation funded project (2020M683355, 2020T150542), the Science and Technology Plan Project of Sichuan Province of China (2021YJ0543) and the Fundamental Research Funds for the Central Universities (2682023KJ002).

Authors' contributions
Xiaopan Lai: Conceptualization, Methodology, Software, Writing–original draft. Zhao Lu: Data analysis. Xinyu Xu: Data analysis. Chuanjin Yu: Conceptualization, Methodology, Project administration.

Funding
This work was financially supported by the China Postdoctoral Science Foundation funded project (2020M683355, 2020T150542), the Science and Technology Plan Project of Sichuan Province of China (2021YJ0543) and the Fundamental Research Funds for the Central Universities (2682023KJ002).

Availability of data and materials
The data that support the findings of this study are available from the corresponding author upon reasonable request.

Competing interests
The authors declare that they have no known competing financial interests or personal relationships that could have appeared to influence the work reported in this paper.

Received: 9 May 2023 Accepted: 1 July 2023
Published online: 25 July 2023

References

Abishek A, Nageswara Rao B (2019) Reliability Study of Railway Bridge Circular Pier Using Monte Carlo Simulation. In: Rao ARM, Ramanjaneyulu K (eds) Recent Advances in Structural Engineering, Volume 2. Springer, Singapore, pp 527–35. https://doi.org/10.1007/978-981-13-0365-4_45

Aydın Z, Ayvaz Y (2013) Overall cost optimization of prestressed concrete bridge using genetic algorithm. KSCE J Civ Eng 17:769–776. https://doi.org/10.1007/s12205-013-0355-4

Chen Z-Q, Zheng S-X, Zhang J, Jia H (2021) Seismic reliability analysis of high-pier railway bridges with correlated random parameters via an improved maximum entropy method. Structures 33:4538–4555. https://doi.org/10.1016/j.istruc.2021.07.039

Deviprasad BS, Saseendran R, Dodagoudar GR (2022) Reliability Analysis of a Bridge Pier Supported on a Rocking Shallow Foundation under Earthquake Loading. Int J Geomechanics 22:04021298. https://doi.org/10.1061/(ASCE)GM.1943-5622.0002287

Fahmy MF, Moussa AM, Wu Z (2023) Precast bridge piers: Construction techniques, structural systems, and seismic response. Adv Struct Eng 26:611–639. https://doi.org/10.1177/13694332221133596
Fu J-Y, Ge X, Li J-T, Sun Z-G, Qian H, Wang D-S (2023) Experimental investigation of the seismic performance of precast post-tensioned segmental bridge piers with stainless energy-dissipating bars. Eng Struct 283:115889. https://doi.org/10.1016/j.engstruct.2023.115889
Ghosh S, Ghosh S, Chakraborty S (2018) Seismic reliability analysis of reinforced concrete bridge pier using efficient response surface method–based simulation. Adv Struct Eng 21:2326–2339. https://doi.org/10.1177/1369433218773422
Hoang PH, Phan HN, Nguyen DT, Paolacci F (2021) Kriging metamodel-based seismic fragility analysis of single-bent reinforced concrete highway bridges. Buildings 11:238. https://doi.org/10.3390/buildings11060238
Mander JB, Priestley MJN, Park R (1988a) Observed Stress-Strain Behavior of Confined Concrete. J Struct Eng 114:1827–1849. https://doi.org/10.1061/(ASCE)0733-9445(1988)114:8(1827)
Mander JB, Priestley MJN, Park R (1988b) Theoretical Stress-Strain Model for Confined Concrete. J Struct Eng 114:1804–1826. https://doi.org/10.1061/(ASCE)0733-9445(1988)114:8(1804)
Mehrsoroush A, Saiidi MS, Ryan K, University of Nevada R (2017) Development of Earthquake-Resistant Precast Pier Systems for Accelerated Bridge Construction in Nevada
Palermo A (2016) Quasi-Static Testing of a 1/3 Scale Precast Concrete Bridge Utilising a Post-Tensioned Dissipative Controlled Rocking Pier
Qu H, Li T, Wang Z, Wei H, Shen J, Wang H (2018) Investigation and verification on seismic behavior of precast concrete frame piers used in real bridge structures: Experimental and numerical study. Eng Struct 154:1–9. https://doi.org/10.1016/j.engstruct.2017.10.069
Safari M, Ghasemi SH, Haj SeiyedTaghia SA (2021) Target reliability analysis of bridge piers concerning the earthquake extreme event limit state. Eng Struct 245:112910. https://doi.org/10.1016/j.engstruct.2021.112910
Shi G, Shi Y, Wang Y (2007) Behaviour of end-plate moment connections under earthquake loading. Eng Struct 29:703–716. https://doi.org/10.1016/j.engstruct.2006.06.016
Shanghai Tunnel Engineering & Rail Transit Design and Research Institute (2021) Technical standard for prefabricated bridge piers of rail transit. DG/TJ 08–2345–2020 J 15506-2021.
Wang Z, Ge J, Wei H, Liu F (2009) Recent Development in Seismic Research of Segmental Bridge Columns. J Earthq Eng Eng Vib 29:147–54. https://doi.org/10.13197/j.eeev.2009.04.007
Wang J, Li F (2022) Numerical Simulation Analysis of the Seismic Performance of Precast Bridge Piers. Math Probl Eng 2022:e6337791. https://doi.org/10.1155/2022/6337791
White S, Palermo A (2016) Quasi-Static Testing of Posttensioned Nonemulative Column-Footing Connections for Bridge Piers. J Bridge Eng 21:04016025. https://doi.org/10.1061/(ASCE)BE.1943-5592.0000872
Zhang Q, Alam MS (2020) State-of-the-Art Review of Seismic-Resistant Precast Bridge Columns. J Bridge Eng 25:03120001. https://doi.org/10.1061/(ASCE)BE.1943-5592.0001620
Zhanghua X, Jiping G, Youqin L, Faqiang Q (2020) Shake table study on precast segmental concrete double-column piers. Earthq Eng Eng Vib 19:705–723. https://doi.org/10.1007/s11803-020-0590-x
Zhao R, Zheng K, Wei X, Jia H, Li X, Zhang Q et al (2022) State-of-the-art and annual progress of bridge engineering in 2021. Adv Bridge Eng 3:29. https://doi.org/10.1186/s43251-022-00070-1

Publisher's Note